IOPscience iopscience.iop.org

Home Search Collections Journals About Contact us My IOPscience

Piezoelectric coefficients of L-histidine hydrochloride monohydrate obtained by synchrotron x-ray Renninger scanning

This article has been downloaded from IOPscience. Please scroll down to see the full text article.

2007 J. Phys.: Condens. Matter 19 106218

(http://iopscience.iop.org/0953-8984/19/10/106218)

View the table of contents for this issue, or go to the journal homepage for more

Download details:
IP Address: 129.252.86.83
The article was downloaded on 28/05/2010 at 16:30

Please note that terms and conditions apply.

IOP PUBLISHING JOURNAL OF PHYSICS: CONDENSED MATTER

J. Phys.: Condens. Matter **19** (2007) 106218 (9pp) doi:10.1088/0953-8984/19/10/106218

Piezoelectric coefficients of L-histidine hydrochloride monohydrate obtained by synchrotron x-ray Renninger scanning

A S de Menezes[1], A O dos Santos[1], J M A Almeida[2], J M Sasaki[2] and L P Cardoso[1]

[1] IFGW, Universidade Estadual de Campinas-UNICAMP, CP 6165, 13083-970-Campinas, SP, Brazil
[2] Departamento de Física, Universidade Federal do Ceará, CP 6030, 60455-760, Fortaleza, CE, Brazil

E-mail: cardoso@ifi.unicamp.br

Received 9 November 2006, in final form 23 January 2007
Published 23 February 2007
Online at stacks.iop.org/JPhysCM/19/106218

Abstract

The method for determining piezoelectric coefficients based on synchrotron radiation x-ray multiple diffraction (Avanci *et al* 1998 *Phys. Rev. Lett.* **81** 5426) has been used in the case of a single crystal of the amino acid L-histidine·HCl·H_2O. The method relates the E-induced strain with the angular shift in the multiple diffraction peak position. Thus, it allowed us to determine all three ($d_{14} = 2.25(9) \times 10^{-10}$ C N^{-1}, $d_{25} = 4.1(5) \times 10^{-11}$ C N^{-1} and $d_{36} = 2.3(2) \times 10^{-10}$ C N^{-1}) piezoelectric coefficients of L-histidine·HCl·H_2O, using the (10 0 0) and (0 0 4) primary reflections.

1. Introduction

L-histidine is an amino acid that is synthesized relatively slowly in the human body, and its deficiency can result in delayed growth and skin eczema. Histidine can exist in two isomeric forms, L-histidine and D-histidine, in which only the L-isomer is bioactive. It can be converted to histamine, which is a major neurotransmitter in the brain and throughout the nervous system. It is essential for tissue growth and repair and, furthermore, it helps to store glucose in the liver. L-histidine residue in enzymes performs a very important function in enzymatic reactions. The dimensions and tautomeric form of the imidazole ring of the molecule are of importance because of the role of this group in coordinating zinc in zinc insulin.

L-histidine·HCl·H_2O ($C_6H_9O_2N_3$·HCl·H_2O) crystallizes in the orthorhombic system, space group $P2_12_12_1$, with four molecules per unit cell, and with the lattice parameters $a = 15.301(3)$ Å, $b = 8.921(2)$ Å and $c = 6.846(2)$ Å [1]; its molecule is in the zwitter ion form.

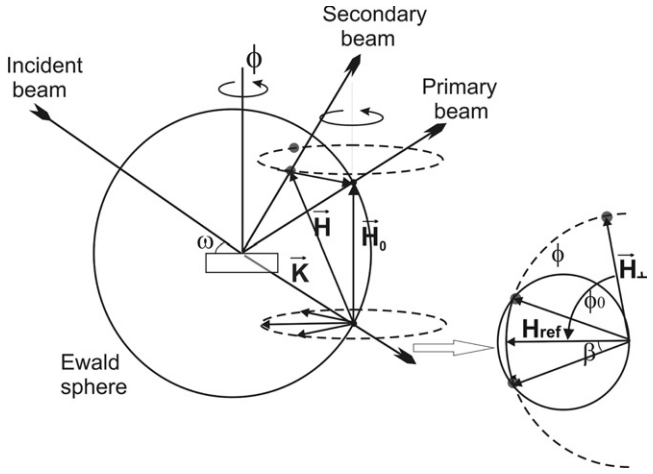

Figure 1. Scheme of a three-beam multiple diffraction case using the Ewald sphere.

The x-ray multiple diffraction (XRMD) technique is a very sensitive and versatile probe with which to detect small lattice deformations, and it has been successfully applied, as a novel method to determine piezoelectric coefficients, in the case of mNA [2] organic single crystal. The method has also been used to provide the required piezoelectric coefficients for other materials such as: MBANP [3], Rochelle salt [4] and also for the amino acid L-arginine·HCl·H_2O [5, 6]. The study of piezoelectric properties of amino acid crystals is completely justified not only for the physics of crystals but also in biophysics [7].

In this study, the XRMD method was applied to an L-histidine·HCl·H_2O single crystal to obtain the all piezoelectric coefficients (d_{14}, d_{25} and d_{36}) of this amino acid crystal. Furthermore, XRMD was also used, by adequately choosing the secondary reflections, to provide the lattice parameters of this crystal.

2. Theory

2.1. Multiple diffraction peak position in a Renninger scan

The multiple diffraction phenomenon arises when an incident beam simultaneously satisfies the Bragg law for more than one set of lattice planes within the crystal. For this, the plane called primary (h_0, k_0, ℓ_0) is adjusted to diffract the incident beam. With the rotation (angle ϕ) of the sample around the primary reciprocal lattice vector, several other planes called secondary (h_s, k_s, ℓ_s) and coupling (h_0–h_s, k_0–k_s, ℓ_0–ℓ_s), will also enter into the diffraction condition simultaneously with the primary plane. These coupling planes establish the interaction between the primary and the secondary reflections. In the pattern of I_{primary} versus ϕ, called a Renninger scan (RS) [8], positive and negative (dip) secondary peaks can appear distributed according to the symmetry of the primary vector, representing the energy transfer from the secondary to the primary reflection (peak) and vice versa (dip), and also considering the symmetry plane established by the ϕ rotation. The secondary peak position in the RS is given by $\phi = \phi_0 \mp \beta'$ and the $\mp$ signal defines the entrance and the exit of the secondary reciprocal lattice point of the Ewald sphere (ES) by rotation. ϕ_0 is the angle between $\mathbf{H}_\perp$ (the component of $\mathbf{H}$ on a plane perpendicular to $\mathbf{H}_0$) and $\mathbf{H}_{\text{Ref}}$, the reference vector, as shown in figure 1. The secondary peak

position equation is a function of the unit cell parameters and it is given by [9]

$$\cos(\beta'_{hk\ell}) = \frac{1}{2}\frac{(H^2 - \mathbf{H}\cdot\mathbf{H}_0)}{\sqrt{\frac{1}{\lambda^2} - \frac{H_0^2}{4}}\sqrt{H^2 - H_{\mathrm{p}}^2}} = f(a, b, c, \alpha, \beta, \gamma, \lambda, \mathbf{H}, \mathbf{H}_0) \tag{1}$$

where $\mathbf{H}_0$ is the primary reciprocal lattice vector, $\mathbf{H}$ is the secondary reciprocal lattice vector, $\mathbf{H_p} = (\mathbf{H}\cdot\mathbf{H}_0)(H_0/H_0^2)$, λ is the wavelength of the incident beam, and ϕ_0 can be obtained from

$$\cos(\phi_0) = \frac{\mathbf{H}_\perp \cdot \mathbf{H}_{\mathrm{Ref}}}{\mathbf{H}_\perp \cdot \mathbf{H}_{\mathrm{Ref}}}. \tag{2}$$

For the orthorhombic crystal, the unit cell vectors are written in an orthogonal frame as

$$\boldsymbol{a} = (a, 0, 0), \qquad \boldsymbol{b} = (0, b, 0) \qquad \text{and} \qquad \boldsymbol{c} = (0, 0, c) \tag{3}$$

and the primary and secondary reciprocal lattice vectors are given by

$$\mathbf{H_0} = \frac{h_0}{a}\hat{\boldsymbol{a}} + \frac{k_0}{b}\hat{\boldsymbol{b}} + \frac{\ell_0}{c}\hat{\boldsymbol{c}} \qquad \text{and} \qquad \mathbf{H}_{hk\ell} = \frac{h}{a}\hat{\boldsymbol{a}} + \frac{k}{b}\hat{\boldsymbol{b}} + \frac{\ell}{c}\hat{\boldsymbol{c}}. \tag{4}$$

In order to determine the lattice parameters, a primary reflection of the type (h_0 0 0) and three secondary reflections (h_1 k_1 l_1), (h_2 k_2 l_2) and (h_3 k_3 l_3) have been chosen to provide three equations of the type

$$\cos(\beta'_{hk\ell}) = \frac{1}{2}\frac{\frac{h(h-h_0)}{a^2} + \frac{k^2}{b^2} + \frac{\ell^2}{c^2}}{\sqrt{\frac{1}{\lambda^2} - \frac{h_0^2}{4a^2}}\sqrt{\frac{k^2}{b^2} + \frac{\ell^2}{c^2}}}, \tag{5}$$

where the equations (4) were substituted into (1). Then, by using these three equations, which are function of the lattice parameters in case of orthorhombic crystals, is possible to solve the system of equations by using a chosen mathematical program. Therefore, among the several solutions of the system it is easy to identify the required L-histidine hydrochloride monohydrate lattice parameters, since the values can be compared to ones published in the literature.

2.2. Application of an external electrical field

The application of a static or quasi-static electrical field to a piezoelectric crystal generates strains in the crystal; this is the well-known converse piezoelectric effect [10]. The piezoelectric tensor, expressed in the matrix form, for the 222 point group is given by

$$\begin{pmatrix} \varepsilon_{xx} \\ \varepsilon_{yy} \\ \varepsilon_{zz} \\ 2\varepsilon_{yz} \\ 2\varepsilon_{xz} \\ 2\varepsilon_{xy} \end{pmatrix} = \begin{pmatrix} 0 & 0 & 0 \\ 0 & 0 & 0 \\ 0 & 0 & 0 \\ d_{14} & 0 & 0 \\ 0 & d_{25} & 0 \\ 0 & 0 & d_{36} \end{pmatrix} \begin{pmatrix} E_X \\ E_Y \\ E_Z \end{pmatrix}. \tag{6}$$

So, equation (6) leads to

$$\varepsilon_{yz} = \tfrac{1}{2}d_{14}E_x, \tag{7}$$

$$\varepsilon_{xz} = \tfrac{1}{2}d_{25}E_y \qquad \text{and} \tag{8}$$

$$\varepsilon_{xy} = \tfrac{1}{2}d_{36}E_z. \tag{9}$$

The ε_{yz}, ε_{xz} and ε_{xy} strains are given by

$$\varepsilon_{yz} = -\tfrac{1}{2}\Delta\alpha, \tag{10}$$

$$\varepsilon_{xz} = -\tfrac{1}{2}\Delta\beta \qquad \text{and} \tag{11}$$

$$\varepsilon_{xy} = -\tfrac{1}{2}\Delta\gamma \tag{12}$$

where $\Delta\alpha$, $\Delta\beta$ and $\Delta\gamma$ are the variations in the α, β and γ unit cell angles induced by the electrical field application. The substitution of equations (10), (11) and (12) into equations (7), (8) and (9), respectively, leads to the d_{14}, d_{25} and d_{36} piezoelectric coefficients:

$$d_{14} = -\frac{1}{E_x}\Delta\alpha, \qquad d_{25} = -\frac{1}{E_y}\Delta\beta \qquad \text{and} \qquad d_{36} = -\frac{1}{E_z}\Delta\gamma. \tag{13}$$

Equation (13) is used in the determination of the L-histidine·HCl·H_2O coefficients.

As to the determination of $\Delta\alpha$, $\Delta\beta$ and $\Delta\gamma$ values, first, the unit cell vectors (equation (3) have to be written for a monoclinic crystal. Thus, by considering the electric field applied in each of the [1 0 0], [0 1 0] and [0 0 1] directions, the three obtained equations (5), for the monoclinic case, depend on the α, β and γ angles, respectively. Therefore, the $\Delta\alpha$, $\Delta\beta$ and $\Delta\gamma$ values can be expressed in terms of the secondary peak position shift ($\Delta\phi$), by differentiating the three peak position equations with respect to α, β and γ, respectively, which gives

$$\Delta\alpha = -\frac{f}{f'_\alpha}\tan(\beta'_{(hk\ell)})\Delta\phi_{(hk\ell)} \tag{14}$$

$$\Delta\beta = -\frac{f}{f'_\beta}\tan\left(\beta'_{(hk\ell)}\right)\Delta\phi_{(hk\ell)} \qquad \text{and} \tag{15}$$

$$\Delta\gamma = -\frac{f}{f'_\gamma}\tan(\beta'_{(hk\ell)})\Delta\phi_{(hk\ell)}. \tag{16}$$

Here, $f = \cos(\beta'_{(hkl)}) = f(a, b, c, \alpha, \beta, \gamma, \lambda, \mathbf{H}, \mathbf{H}_0)$ as defined by equation (1) in a general form, and f' stands for the derivative of f with respect to each corresponding variable (α, β or γ). Therefore, the f/f' ratios used are given as

$$\frac{f}{f'_\alpha} = -\frac{[a + b\cos(\alpha)]\sin(\alpha)}{b + c\ \cos(\alpha)} \tag{17}$$

$$\frac{f}{f'_\beta} = \frac{[-a^2 + 4c^2 + 3ac\ \cos(\beta)]\sin(\beta)}{-3ac + (a^2 - 4c^2)\ \cos(\beta)} \tag{18}$$

$$\frac{f}{f'_\gamma} = \frac{[-2a^2 + 3c^2 + ac\ \cos(\gamma)]\sin(\gamma)}{-ac + (2a^2 - 3c^2)\ \cos(\gamma)} \tag{19}$$

for equations (14), (15) and (16), respectively.

3. Experimental details

L-histidine·HCl·H_2O single crystals were grown by a slow evaporation method using a good seed crystal keeping a constant temperature of 23 °C. In order to characterize the powdered samples well, x-ray diffraction data were collected with a Philips X'Pert MRD diffractometer operating at 40 kV/40 mA, using Cu Kα radiation and a pyrolytic graphite diffracted beam monochromator. The diffraction patterns were obtained with a step size of 0.02° (2θ) and with a counting time of 12 s step^{-1}. A sample oscillation condition was used to minimize preferred orientation effects. The Rietveld refinement program DBWS9807 [11] was used and the measurements were carried out in the angular range 10°–55° (2θ). The refined parameters were as follows: scale factor, 2θ-zero point, four coefficients to describe the functional dependence of the background, three cell dimensions (a, b and c), three half-width parameters, two parameters to describe the 2θ-dependence of the pseudo-Voigt (pV) profile shape function, asymmetric factor, 39 atomic coordinates and 13 isotropic atom displacement (temperature) parameters. Table 1 shows the refined values for the atomic coordinates as well as the isotropic thermal parameters. The last variable to be refined was the preferred orientation parameter.

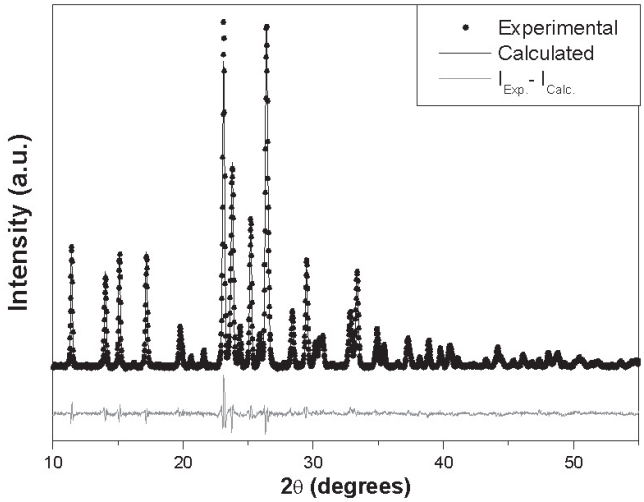

Figure 2. The final Rietveld refinement plot. The R-factors are $R_{wp} = 8.05\%$, $R_{Bragg} = 3.88\%$ and $S = 2.06$.

Table 1. L-histidine·HCl·H_2O atomic coordinates and isotropic thermal parameters obtained from the Rietveld refinement.

	x	y	z	B
C(1)	0.374(2)	0.183(2)	0.476(3)	2.9(8)
C(2)	0.411(1)	0.098(3)	0.295(4)	3.3(9)
C(3)	0.459(1)	0.219(3)	0.179(2)	0.0
C(3)	0.4027(4)	0.3658(9)	0.141(2)	9.4(9)
C(5)	0.3428(4)	0.5300(9)	0.940(2)	6.9(9)
C(6)	0.3680(4)	0.4798(9)	0.248(2)	2.1(8)
N(1)	0.324(1)	0.038(2)	0.218(2)	5.8(7)
N(2)	0.3846(4)	0.4000(9)	0.949(2)	3.1(7)
N(3)	0.3313(4)	0.5804(9)	0.124(2)	6.1(7)
O(1)	0.291(1)	0.193(2)	0.539(3)	8.5(7)
O(2)	0.415(1)	0.275(1)	0.623(2)	9.3(6)
O(3)	0.0868(7)	0.108(1)	0.404(2)	7.9(7)
Cl	0.1743(5)	0.2256(5)	0.025(1)	7.8(3)

Figure 2 displays the comparison between the observed and the calculated diffraction patterns and the R-factor values $R_{Bragg} = 3.88\%$, $R_{wp} = 8.05\%$ and $S = 2.06$ (goodness of fit) were obtained from the refinement.

Three single crystals were cut, from the same piece, into parallelepipeds to apply the electric field in the a, b and c directions, with dimensions of 1.6 mm × 4.4 mm × 3.0 mm, 3.2 mm × 2.4 mm × 7.5 mm and 2.5 mm × 4.5 mm × 2.2 mm, respectively. Also, in this case, the versatility of the XRMD method for piezoelectric coefficient determination was not used since the samples were cut in specific directions (a, b and c-axes), which facilitates the sample preparation very much. The electric field was applied in the larger face and the x-ray incident beam reached the smaller sample face. The electric field was generated by a variable-voltage low-current DC power supply. Silver electrodes were painted on the larger face of the crystal and the field was applied via wires running from the power supply to the sample [6].

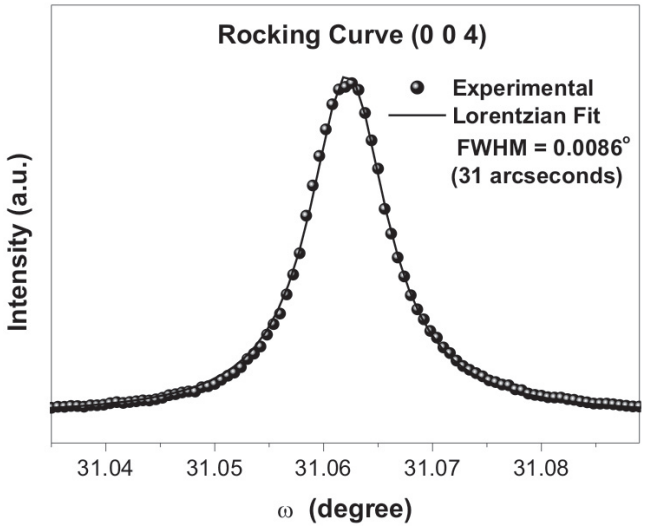

Figure 3. Rocking curve for the (0 0 4) reflection of the L-histidine·HCl·H_2O sample.

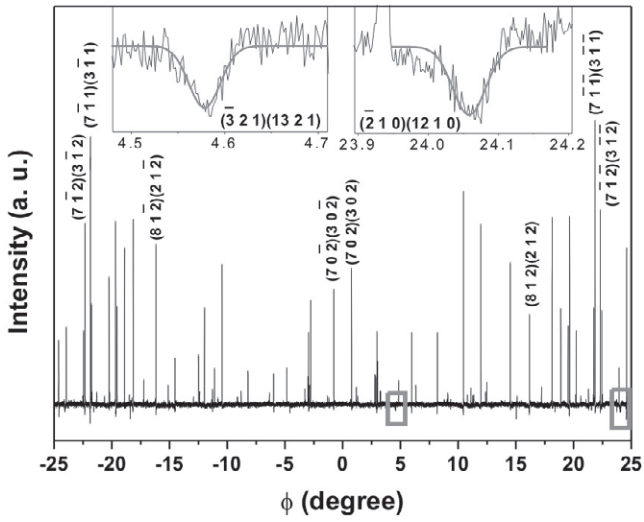

Figure 4. Portion of the (10 0 0) RS around the $\phi = 0°$ symmetry mirror of L-histidine·HCl·H_2O. Inset: details of two of the three multiple diffraction cases (dips) involved in the lattice parameter determination.

RSs for all samples were carried out at station XRD1 of the National Synchrotron Light Source (LNLS), Campinas, SP, Brazil. The wavelengths used in the two beam times of our experiments were 1.5387(1) Å and 1.7667(1) Å for lattice parameter determination and electrical field application (piezoelectricity). A beam size of the order of 1.0 mm × 1.0 mm was defined on the sample surface. The Huber three-axis diffractometer used in the experiments is mounted at station XRD1 of the LNLS, and provides high-resolution measurements with step sizes of 0.0002° (ϕ-*axis*) and 0.0005° (ω-*axis*).

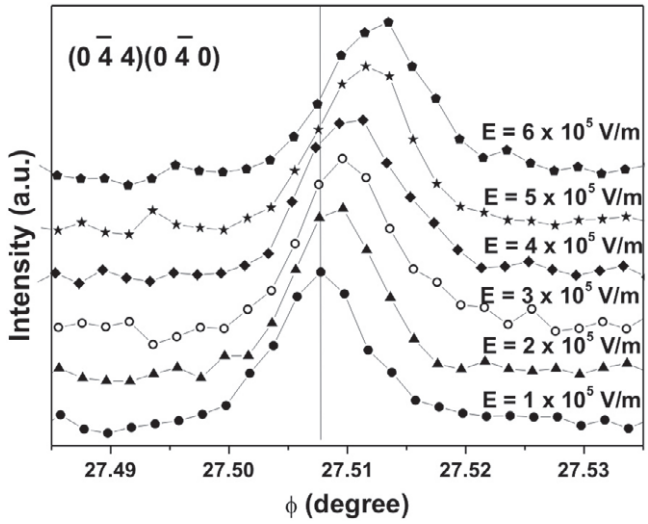

Figure 5. Angular shift in the $(0\bar{4}4)(0\bar{4}0)$ secondary peak position as a function of the applied electric field.

Table 2. The obtained L-histidine·HCl·H_2O lattice parameters.

	a (Å)	b (Å)	c (Å)
Oda and Koyama	15.301(3)	8.921(2)	6.846(2)
Rietveld	15.3067(7)	8.9266(4)	6.8499(4)
XRMD	15.3143(9)	8.931(2)	6.857(8)
Secondary reflections used to calculate the lattice parameters ($\lambda = 1.5387(1)$ Å)			
hkl	$(\bar{4}\ 3\ 0)(14\ 3\ 0)$	$(\bar{2}\ 1\ 0)(12\ 1\ 0)$	$(\bar{3}\ 2\ 1)(13\ 2\ 1)$
ϕ (deg)	21.313(1)	24.054(2)	4.576(2)
β' (deg)	1.313	24.054	37.6782

4. Results and discussion

Regarding the experiments with the L-histidine·HCl·H_2O single crystals, figure 3 shows the rocking curve for the (0 0 4) primary reflection and the FWHM obtained was 31 arc sec, which indicates a good crystallographic quality. The FWHM obtained for a (2 2 2) standard Si sample was 15 arc sec.

Figure 4 shows a typical $\phi = 0°$ symmetry mirror region of the RS for L-histidine·HCl·H_2O (10 0 0), although all regions around $\phi = 0°$ and 90° symmetry mirrors have been measured in the experiments. The indexing of the secondary peaks was made using the UMWEG program [12]. The three secondary reflections used in the calculation of the lattice parameters were the four-beam cases $(\bar{4}\ 3\ 0)(14\ 3\ 0)$, $(\bar{2}\ 1\ 0)$ (12 1 0) and $(\bar{3}\ 2\ 1)$ (13 2 1). These reflections were chosen since they have small β' values within the measured RS range, i.e., the adequate condition for lattice parameter determination using this wavelength (1.5387 Å).

The lattice parameters obtained by the XRMD method and the β' values for the secondary reflections detected in the measured Renninger scan region that were used are given in table 2. Also, this table shows the values obtained from the Rietveld method as well as those obtained

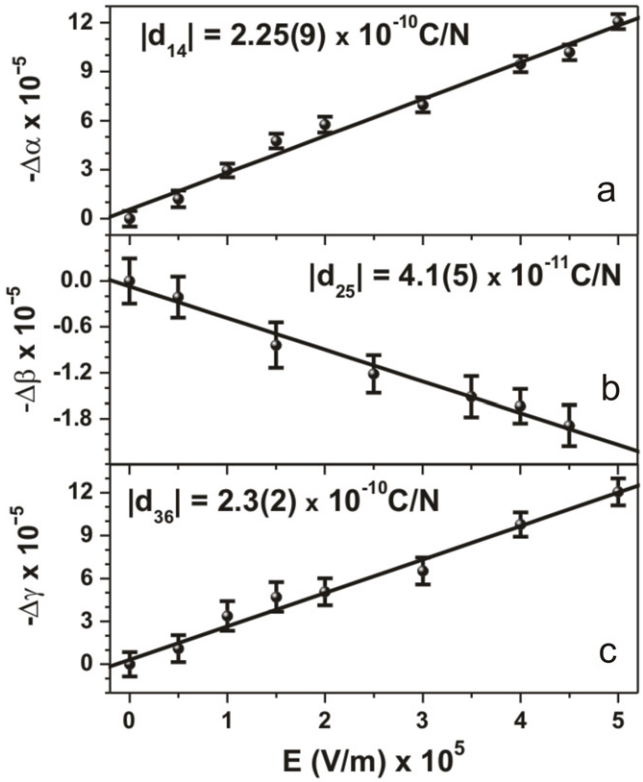

Figure 6. L-histidine·HCl·H_2O lattice strain as a function of the applied electric field to provide the piezoelectric coefficients. Reflections used for XRMD: (a) primary (0 0 4) and secondary (0 $\overline{4}$ 4) for d_{14} coefficient, (b) (10 0 0) and (2 0 $\overline{2}$) for d_{25} and (c) (10 0 0) and (4 $\overline{4}$ 0) for d_{36}.

from the literature for comparison purposes. Prior to the electric field measurements, the L-histidine·HCl·H_2O lattice parameters were redetermined for the wavelength used (1.7667 Å). Even though the conditions were not adequate for the lattice parameter determination, the values presented in table 2 for each unit cell parameter are within the larger standard deviation of the redetermined values.

For the field applied towards the *b*-axis and the *c*-axis, the (10 0 0) primary reflection and the (2 0 $\overline{2}$)(8 0 $\overline{2}$) and (4 $\overline{4}$ 0)(6 $\overline{4}$ 0) secondary reflections were used, respectively, whereas for the field applied towards the *a*-axis, (0 0 4) and (0 $\overline{4}$ 4)(0 $\overline{4}$ 0) reflections were used as primary and secondary, respectively. These secondary reflections were measured in the two sides of the symmetry mirror, allowing for the correction of the symmetry mirror position. The shifts, due to the E application, in the peak positions of the three above-mentioned four-beam cases were transformed into lattice strains through equations (14), (15) and (16), respectively. In figure 5, as an example of this shift, the effect of the applied electric field in the (0 $\overline{4}$ 4)(0 $\overline{4}$ 0) peak position is presented. Using equations (13) is possible to obtain the d_{14}, d_{25} and d_{36} coefficients.

Figure 6(a) shows the graph of $-\Delta\alpha$ versus E_x, which yields the coefficient $|d_{14}| = 2.25(9) \times 10^{-10}$ C N^{-1}. Figure 6(b), $-\Delta\beta$ versus E_y, gives rise to the coefficient $|d_{25}| = 4.1(5) \times 10^{-11}$ C N^{-1} and figure 6(c), $-\Delta\gamma$ versus E_z, provides the coefficient $|d_{36}| = 2.3(2) \times 10^{-10}$ C N^{-1}.

$$\begin{array}{c} \\ \bar{E}_x \\ \bar{E}_y \\ \bar{E}_z \end{array} \begin{array}{c} \begin{array}{cccccc} [100] & [010] & [001] & [011] & [101] & [110] \end{array} \\ \begin{pmatrix} 0 & 0 & 0 & 225(9) & 0 & 0 \\ 0 & 0 & 0 & 0 & 41(5) & 0 \\ 0 & 0 & 0 & 0 & 0 & 230(20) \end{pmatrix} \end{array} pC/N$$

Figure 7. Complete piezoelectric tensor of L-histidine·HCl·H_2O obtained by the x-ray multiple diffraction method in this work.

Finally, the complete piezoelectric tensor obtained for L-histidine·HCl·H_2O using the XRMD method is presented in figure 7.

5. Conclusions

The method of determining the piezoelectric coefficients based on the XRMD technique using synchrotron radiation was successfully applied to L-histidine hydrochloride monohydrate crystal. As far as we know, this is the first determination of all piezoelectric coefficients of this amino acid and it represents a useful contribution to its piezoelectric characterization since quantitative data are required for technological applications and also for theoretical modelling. Furthermore, the technique was also used in the sample lattice parameter determination with adequate choice of the secondary peaks in the Renninger scan, and the results are in very good agreement with those published in the literature.

Acknowledgments

The authors thank the Brazilian Agencies CNPq, CAPES and are grateful for support from the Laboratório Nacional de Luz Síncrotron (LNLS), Campinas, SP, Brazil.

References

[1] Oda K and Koyama H 1972 *Acta Crystallogr.* B **28** 639
[2] Avanci L H, Cardoso L P, Girdwood S E, Pugh D, Sherwood J N and Roberts K J 1998 *Phys. Rev. Lett.* **81** 5426
[3] Avanci L H, Cardoso L P, Sasaki J M, Girdwood S E, Roberts K J, Pugh D and Sherwood J N 2000 *Phys. Rev.* B **61** 6507
[4] dos Santos A O, Yaegashi W H, Marcon R, Li B B, Gelano R V, Cardoso L P, Sasaki J M, Miranda M A R and Melo F E A 2001 *J. Phys.: Condens. Matter* **13** 10497
[5] Almeida J M A, Miranda M A R, Remédios C M R, Melo F E A, Freire P T C, Sasaki J M, Cardoso L P, dos Santos A O and Kycia S 2003 *J. Appl. Crystallogr.* **36** 1348
[6] Almeida J M A, Miranda M A R, Avanci L H, de Menezes A S, Cardoso L P and Sasaki J M 2006 *J. Synchrotron Radiat.* **13** 435
[7] Lemanov V V 2000 *Piezoelectric Materials: Advances in Science, Technology and Applications* ed C Galassi *et al* (Dordrecht: Kluwer) p 1
[8] Renninger M 1937 *Z. Phys.* **106** 141
[9] Cole H, Chambers F W and Dum H M 1962 *Acta Crystallogr.* **15** 138
[10] Nye J F 1957 *Physical Properties of Crystals* (Oxford: Oxford Science Publications, Clarendon)
[11] Young R A, Sakthivel A, Moss T S and Paiva-Santos C O 1995 *J. Appl. Crystallogr.* **28** 366
[12] Rossmanith E 2003 *J. Appl. Crystallogr.* **36** 1467